Molecular Crystals and Liquid Crystals
Publication details, including instructions for authors and subscription information:
http://www.tandfonline.com/loi/gmcl18

Electro-Optic Characteristics of Charge-Transfer-Complex Doped Ferroelectric Liquid Crystal Device: Realization of Very High Contrast Ratio and Perfect Bistability

B. Y. Zhang [a], M. Yoshida [a], H. Maeda [a], M. Kimura [a], H. Sekine [a] & S. Kobayashi [a]
[a] Division of Electronic and Information Engineering, Graduate School of Technology, Tokyo University of Agriculture and Technology, Koganei, Tokyo, 184, Japan
Version of record first published: 24 Sep 2006.

To cite this article: B. Y. Zhang , M. Yoshida , H. Maeda , M. Kimura , H. Sekine & S. Kobayashi (1991): Electro-Optic Characteristics of Charge-Transfer-Complex Doped Ferroelectric Liquid Crystal Device: Realization of Very High Contrast Ratio and Perfect Bistability, Molecular Crystals and Liquid Crystals, 202:1, 149-162

To link to this article: http://dx.doi.org/10.1080/00268949108035666

Mol. Cryst. Liq. Cryst., 1991, Vol. 202, pp. 149–162
Reprints available directly from the publisher
Photocopying permitted by license only

Printed in the United States of America

Electro-Optic Characteristics of Charge-Transfer-Complex Doped Ferroelectric Liquid Crystal Device: Realization of Very High Contrast Ratio and Perfect Bistability

B. Y. ZHANG, M. YOSHIDA, H. MAEDA, M. KIMURA, H. SEKINE and S. KOBAYASHI

Division of Electronic and Information Engineering, Graduate School of Technology, Tokyo University of Agriculture and Technology, Koganei, Tokyo 184, Japan

(Received July 25, 1990)

A surface stabilized ferroelectric liquid crystal electro-optic device using FLC material doped with a charge-transfer-complex (CTC), TMTFF-ODTCNQ, was shown to reveal a perfect bistability yielding a 100% memory capability with an inverted polarity accompanying a high contrast ratio reaching 55:1.

The relationship between the EO characteristics and the dynamics of the ions of CTC has been investigated to understand this peculiar EO performance. It was shown that the inverted bistability is caused by the formation of strong internal depolarization field originated from the ions of the CTC molecules accumulating in the interfacial region.

Both the values of the depolarization field and the mobility of ions were evaluated. The value of the former was shown to reach several volts and that of the latter was 5×10^{-7} cm^2/V · s. These values are thought to be enough to cause the inverted bistability phenomena.

Keywords: ferroelectric LC, charge-transfer-complex, inverted bistability

1. INTRODUCTION

Currently, a lot of papers on the surface stabilized ferroelectric liquid crystal (SSFLC) electrooptic (EO) devices[1] have been published by many researchers for their interesting characteristics featured by bistability and fast respond speed.[2]

However, there still exist difficulties in the preparation of the device exhibiting a perfect bistability with a good contrast ratio without containing defects.

Some proposals and demonstrations that provide resolutions for realizing a perfect bistability have been made: the one is to use ultrathin films such as polyimide (PI) Langmuir-Blodgett films[3] for the molecular orientation; the other is to use electrically conductive orientation films[4]; a method which is alternative to above two methods is to use a charge-transfer-complex (CTC)-doped FLC material together with ordinary rubbed PI film; however, in this case the polarity of the EO performance is inverted in the sense that the response is build up immediately after the ceasing of the writing/erasing voltage pulses.[5]

The present work has been done with the aim of giving a quantitative explanation for the mechanism of this inverted bistability. In this work, experiments have been done on the electrical transport properties of the CTC-doped FLC medium in order to understand its effect on the EO characteristics.

From the results of this work, it was concluded that the inverted bistability was caused by the formation of strong internal depolarization fields originating from the ionic charges of the CTC molecules accumulating in the interfacial regions. The value of the depolarization field was determined from the behavior of the inversion currents for triangular voltage waveforms. The mobility of the ionic charges was determined to be 5×10^{-7} cm^2/V · s which is sufficient to cause the inverted bistability when the amount of the doped CTC is appropriate.

Some parts of these analyses were done by referring to the analytical research of Yang and his colleagues[6,7] who dealt with ionic effects on the EO performance of SSFLCDs.

2. EXPERIMENTAL

The structure of the SSFLC cell is the same as that was described in the previous work[5]: the FLC material, ZLI-3654 (E. Merck), was doped with a CTC, TMTTF-ODTCNQ (type LOC-1, supplied from Japan Carlit), whose chemical structure is shown in Figure 1; and then it was filled in a narrow space between two glass plates whose inner surfaces were coated with ITO films which were also covered with ordinary polymide layers (RN305, Nissan Chem. Ind.) rubbed in advance. Typical thickness of the FLC medium was 2 μm.

The amount of the doped CTC ranged from 0.001 to 1.200 wt%; in order to ensure the homogeneity of the dissolved CTC in an FLC host, the mixture was first heated up and kept at 90°C for several minutes then it was cooled down to room temperature for preparing to use.

A uniform and defect free FLC device was prepared by filling the CTC-doped FLC at a temperature that the medium took its isotropic phase and cooling down the cell slowly at the rate of 0.1°C/min; for conducting this procedure a temperature controlling system purchased form Mettler was used. Furthermore, we applied an AC voltage with 40 volts peak-peak (depending on the medium thickness) in high frequency region (1 ~ 100 KHz) to the cell for several minutes in advance before the sample was tested; this process was extremely effective in removing zig-zag defects.

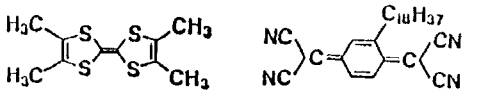

TMTTF ODTCNQ

FIGURE 1 Chemical structure of the CTC named tetramethyltetrathia fuluvalene-octadecyl tetracyanoquinodimethane (TMTTF-ODTCNQ).

Both the EO and electrical characteristics have been measured utilizing a computerized system.

The values of the memory capability and contrast ratio are given in terms of the luminance factors according to CIE 1931 representation on the basis of transmission spectra of the SSFLCD media. The definitions of the memory capability and the contrast ratio are given in the previous paper.[4]

3. RESULTS AND DISCUSSIONS

3.1 Electrooptic Responses

As a result of the treatment with application of the AC field all the zig-zag defects were eliminated from the region of the test pad having an area of 1 cm^2, actual evidence of this effects being shown in Figure 2 (A), (B) and (C), microphotographs, taken before, 5 minutes and 10 minutes after this treatment, respectively. As shown in Figure 2 the microphotograph of (C) exhibits an almost completely zig-zag defect free area observed under crossed polarizers.

The electrooptic responses of a CTC-doped FLC cell, which was prepared with the method as described in the previous section, to the writing/erasing voltage pulses (Figure 3(A)) is shown in Figure 3(B), which is featured by a perfect bistability, having inverted polarity and giving a very high contrast ratio reaching to 55:1. This kind of performance was obtained for the pulse voltages with a width exceeding 200 μs. For comparison, other two extreme examples of EO performance are shown on the same figure; the one is that for a sample using a FLC without doping with CTC but adopting ordinary rubbed polyimide (PI) orientation films (Figure 3(C)), and the other is that for a sample using a CTC doped FLC but adopting PI Langmuir-Blodgett orientation films (Figure 3(D)). In the former a degradation in the memory state is recognized, whereas the latter exhibits a perfect and normal bistability in spite of using a CTC-doped FLC.

The microphotographs of the memory states of this particular sample are shown on Figure 4 (A) and (B), corresponding to the light and dark state, respectively. As shown in Figure 4 the microphotograph of (B) exhibits an almost complete dark state in the configuration of the crossed polarizers. Table I shows the values of the memory capability and contrast ratio of SSFLCDs which were prepared under the same conditions except for changing the CTC dopant in the range 0 to 1.220 wt%. Clearly, the EO performance of the CTC-doped SSFLCD is better than that of the undoped one.

3.2 The Ionic Transient Currents

As the electrical transport of the ionic charge of the CTC dissolved in the FLC host was considered to affect the EO characteristic of the cell, we investigated the transient currents in response to reversal of the applied voltage. Results are shown in Figure 5; the curves for the currents comprise the following three parts: a sharp spike appearing first that originates from the ordinary dielectric relaxation; it is followed by a peak originating from the reversal of the spontaneous polarization,

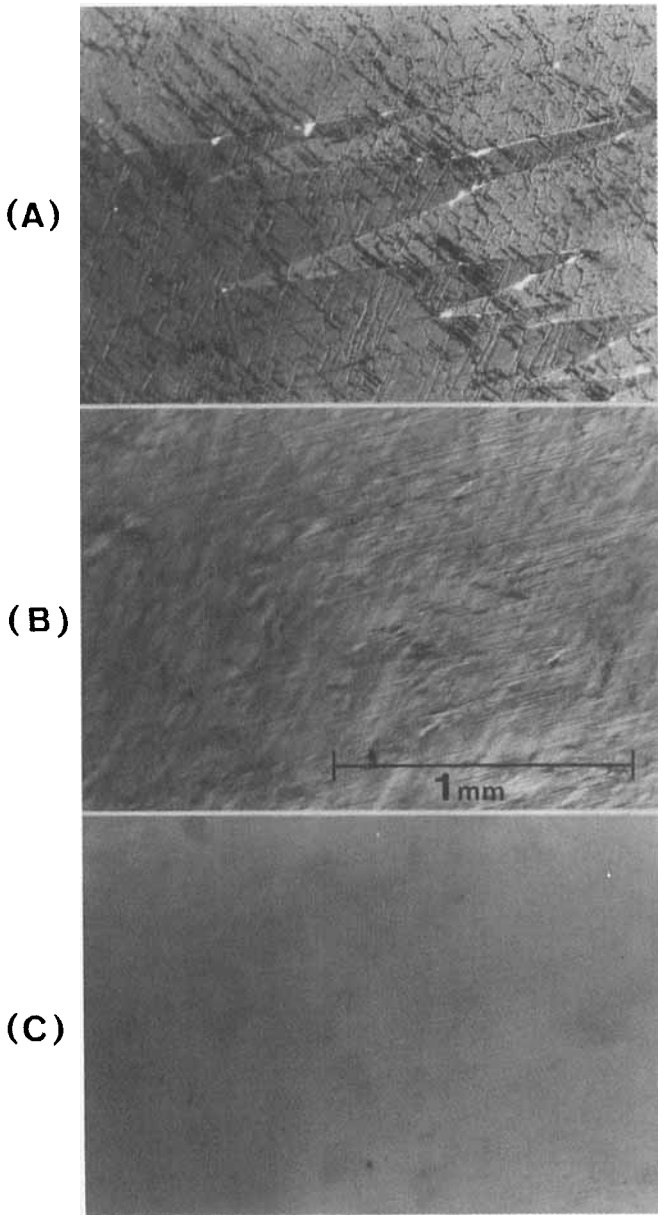

FIGURE 2 Microphotographs of a CTC-doped SSFLCD before (A), 5 minutes (B) and 10 minutes (C) after the treatment of applying triangular wave-form voltage.

then there appears a hump as the final event. This hump is considered to be attributable to the dynamics of the ionic charges.[8] The appearance of this hump depends on the applied voltage as shown in Figure 6. No such a hump was observed for a sample FLC without the CTC doping.

We interpret the time for the peak of the hump, T_h, as the transient time of the

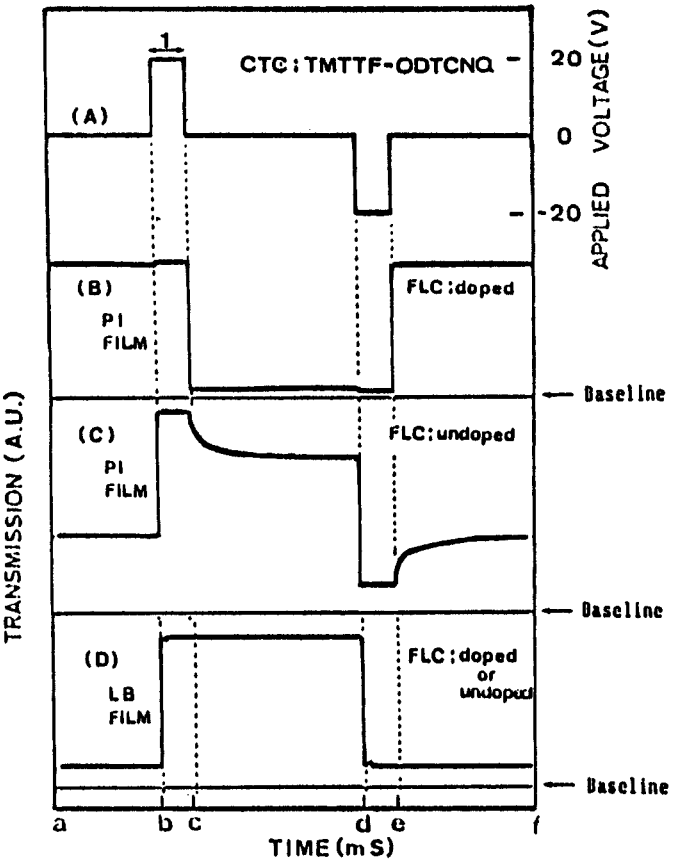

FIGURE 3 Electrooptic response of TMTTF-ODTCNQ doped (B) and undoped (C) SSFLC cells having ordinary rubbed polyimide orientation films, and (D) having polyimide Langmuir-Blodgett orientation films, where (A) is the applied voltage waveform.

ions in the space between two electrodes. Figure 7 shows a plot of T_h versus the reciprocal of the voltage; the dots are drawn by transferring data from those of Figure 6. The data shows a straight line.

An analytical form of T_h may be expressed as

$$T_h = \frac{d^2}{\mu V},$$

where d, μ, and V stand for the spacing between two electrodes, the mobility of the ions, and the voltage across the two electrodes.

From the data of Figure 7, we can obtain $\mu = 5 \times 10^{-7}$ cm^2/V · s.

3.3 An Interpretation of the Inverted Bistability and Evaluation of the Depolarization Field

The carriers of the electrical conduction are ions of the CTC dissolved in the FLC matrix which obey the equilibrium equation:

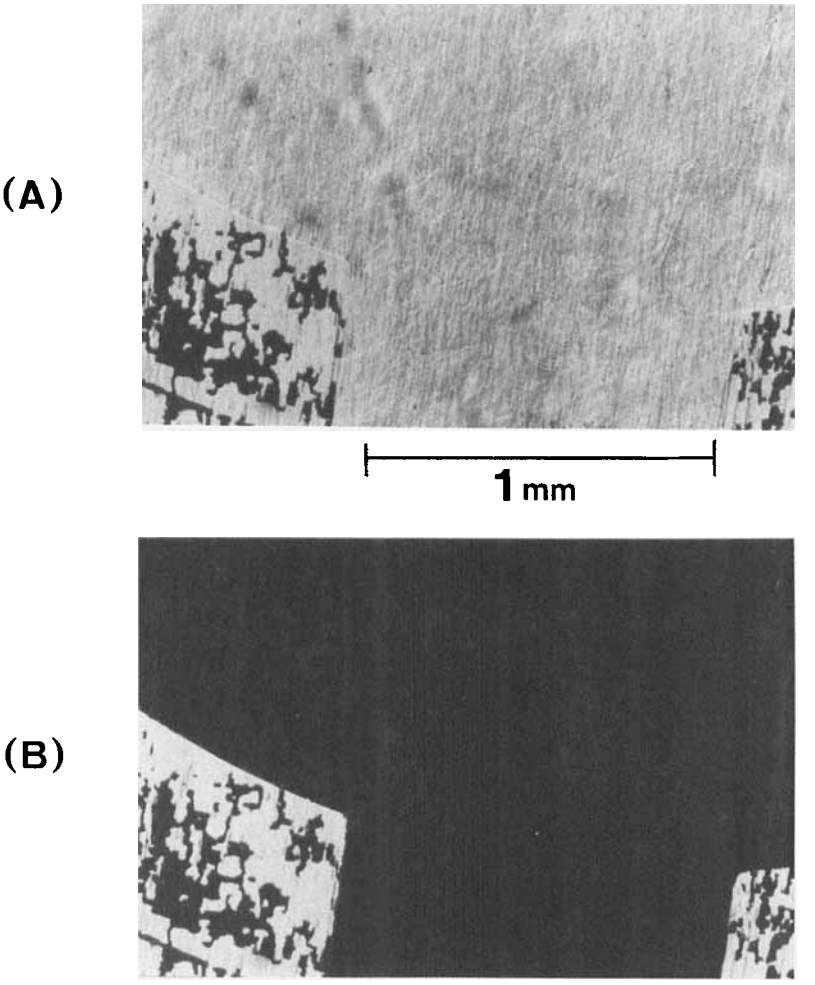

FIGURE 4 Microphotograph of a CTC-doped SSFLC cell (Maximum contrast ratio is 55:1), where the major parts of these photos show the optical states in the electrode pad, (A) and (B), corresponding to the light and dark state, respectively.

$$D + A \rightleftharpoons D^+A^- \underset{K_r}{\overset{K_d}{\rightleftharpoons}} D^+ + A^-, \tag{1}$$

where, D^+A^-, D^+ and A^- are the concentrations of the donor-acceptor pairs, positive (donor) and negative (acceptor) ions of the CTC, respectively.

Under the applied electric field E, the concentration of ions may be governed by the following equation:

$$\frac{dn(t)}{dt} = K_dC - K_rn^2(t) - \frac{E(\mu^+ + \mu^-)}{2d} n(t), \tag{2}$$

TABLE I

Sample No:	Gap [μm]	Dopant (wt%)	Contrast	M (%)
241	2.4	0.083	25.0	100
243	1.7	0.083	31.8	100
238	1.9	0.047	55.2	100
236	2.2	0.083	55.0	100
235	2.4	0.083	14.9	91.9
233	1.8	0.083	26.3	100
240	1.7	0.047	25.6	100
234	2.2	0.083	25.3	100
250	1.6	0.600	14.6	92
257	1.8	0.083	33.7	100
116	1.9	1.220	35.8	100
115	1.9	0.600	33.4	100
113	2.6	0.278	33.5	100
117		0.001	2.2	44.5
118	3.5	Undoped	2.5	48
253	2.3	—	1.6	25.8
242	2.5	—	1.7	28.1
237	2.5	—	4.0	68.8

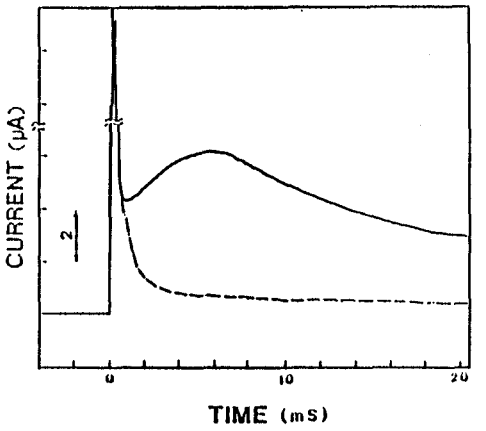

FIGURE 5 Transient current versus time curves for the FLC compound ZLI-3654 doped with CTC of TMTTF-ODTCNQ under applied voltage, V_{p-p}, which is peak to peak of the square waveform voltage. The solid and dashed lines represent the current through the CTC-doped and the undoped SSFLC cells.

where $n(t)$ is the concentration of the dissolved CTC in an ionic form as a function of time ($n(t) = n^+(t) = n^-(t)$ because TMTTF-ODTCNQ is 1:1 complex), and C, μ^+, μ^-, K_d, and K_r stand for the present solute (dopant) concentration, the positive and negative ionic mobility, the dissociation and recombination kinetic constants, respectively.

By introducing the average value of $\mu = (\mu^+ + \mu^-)/2$, the rate Equation (2) can be rewritten as:

$$\frac{dn(t)}{dt} = K_d C - K_r n^2(t) - \frac{E\mu}{d} n(t). \tag{3}$$

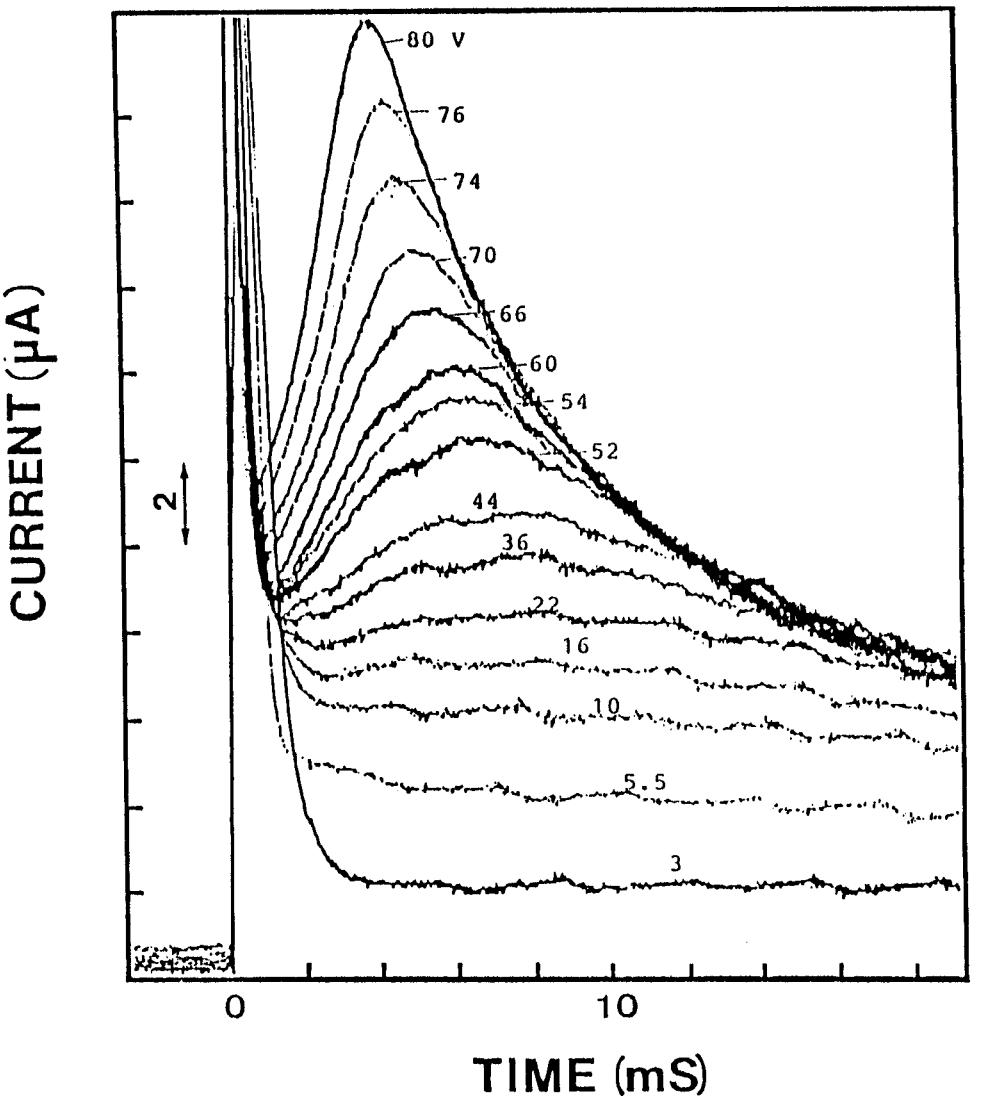

FIGURE 6 Variation of the ionic reversal transient current under the different applied fields at room temperature.

The solution of Equation (3) gives the chemical relaxation time T_R for $E = 0$ as:

$$T_R = \frac{1}{2}(K_r K_d C)^{-1/2}. \tag{4}$$

The electrical relaxation time T_T that is equivalent to the transit time is given by taking only the third term (neglecting both the first and the second terms) of

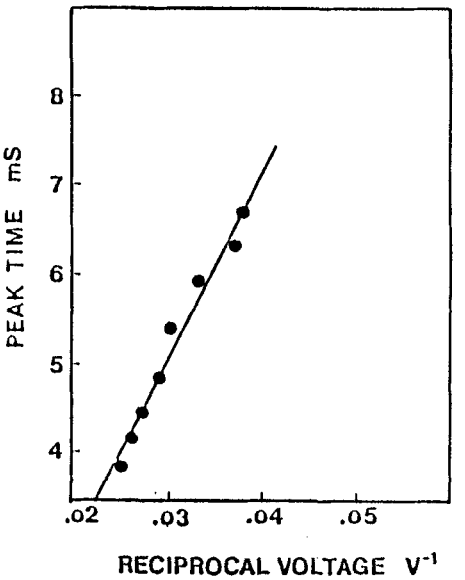

FIGURE 7 Variation in ion hump peak time of Figure 6 as a function of the reciprocal applied voltage.

Equation (3) as

$$\frac{dn(t)}{dt} = -\frac{\mu E}{d} n(t). \tag{5}$$

The solution of Equation (5) gives:

$$T_T = \frac{d}{\mu E}. \tag{6}$$

Usually, $T_R >> T_T$ and the electrolysis rate is much faster than the recombination rate under a high electric field.[9] This situation thought to be valid for the system of CTC-doped-FLC.

Schematic illustrations of the electrical states occurring in a CTC-doped-FLC cell during the application of, e.g., writing voltage and just after switching off this voltage are given in Figure 8 (A) and (B), respectively. In the former, the spontaneous polarization P_s aligns along to the direction of the external applied field E_{appl}; at the same time there build up the following three kinds of the internal depolarization fields: one originating from the accumulated ions of the CTC, E_C; the second originating from the impurity ions, E_I; and the final one originating from spontaneous polarization of FLC, E_P.

In our sample, E_C dominates over other two fields when the concentration of CTC exceeds 0.005–0.600 wt%.[10,11] Just after the switching off the applied external

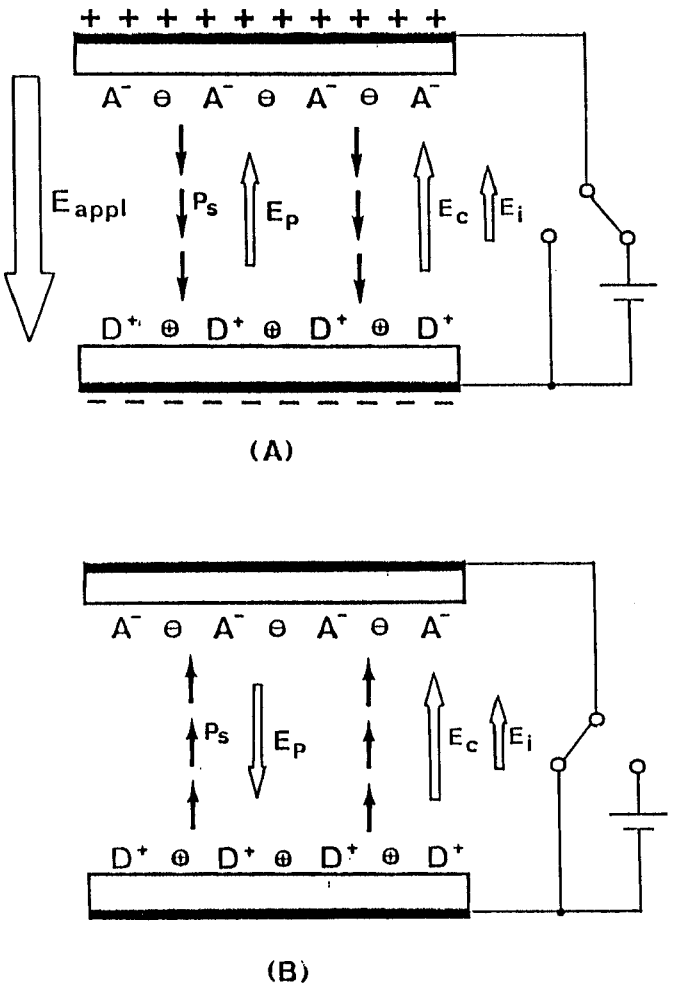

FIGURE 8 Inverted bistability model for TMTTF-ODTCNQ doped SSFLCD.

field, the same charges induced in the electrodes disappear due to the discharge in term of the external circuit having a low impedance of 50 ohms, however, the field E_C lasts meanwhile and it is capable of switching the P_S in the opposite direction as shown in Figure 8 (B); this is a model proposed in this paper for explaining the inverted bistability. No such inverted BS was observed for a CTC-doped FLC when PI-LB films were adopted for the molecular orientation (Figure 3 (D)). This effect can be explained by the neutralization of all the charges accumulating in the region due to the very thinness of the LB films (2 nm). For this reason, the ions of CTC play the key role in realizing the inverted BS by cooperating with the non conductive nature of the orientation films.

The magnitude of the depolarization field can be determined directly by observing the voltage, V_{LC}, which appears just after the removal of the external voltage,

across the LC medium, expressed by

$$V_{LC} = \frac{C_{OR}}{2C_{LC} + C_{OR}} V_{\text{appl.}},$$

where C_{OR} and C_{LC} stand for the capacitance of the orientation films and that of the LC medium. In the case of FLC device the ratio $C_{OR}/C_{LC} = 10^3$, therefore, $V_{LC} = V_{\text{appl.}}$

However, in this paper we determined the depolarization field by comparing the temporal behaviors of reversal currents responding to the triangular waveforms for both the CTC doped and undoped FLCs. The depolarization field E_c, originating from the ions of the CTC, is given by

$$E_c = E_{LC}(\text{doped}) - E_{LC}(\text{undoped}).$$

An example of these reverse currents are shown in Figure 9. For a triangular waveform (trace (A)), the currents for doped (trace (B)) and undoped (trace (C))

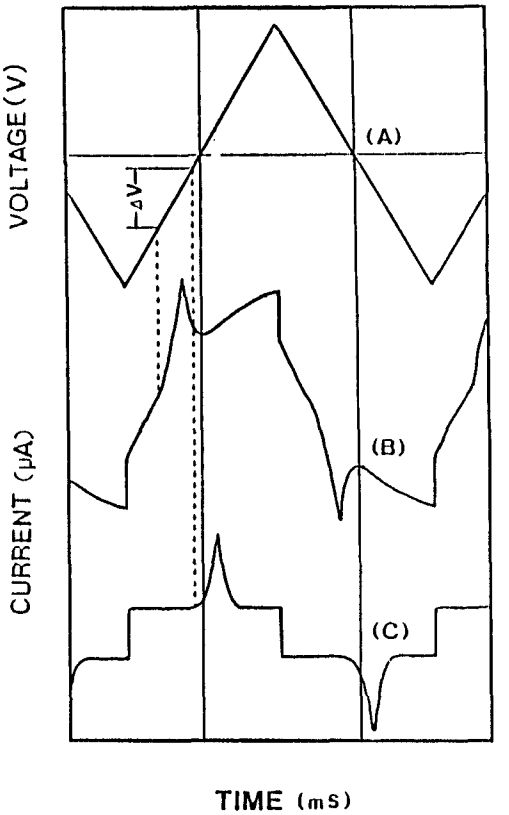

FIGURE 9 Transient current response from triangular wave driving voltage (A), (B) and (C) are, respectively, the current through CTC-doped SSFLCD and undoped one with the same thickness at 20 Hz.

FLCs using rubbed polyimide orientation film (RN 305) are shown; the peaks for the latter appear after those for the doped sample appear. The half value width of the reversal currents for both samples are almost the same. A plot of ΔV versus the frequency is shown in Figure 10 by transferring data from Figure 9. In the extremity of low frequency ΔV reaches 16 volts.

The difference ΔV is indicated also in Figure 11. The instant for the appearance of the peak current depend both on the formation of the depolarization field and on the viscosity of the FLC medium. The effect of the latter can be removed by measuring the current using a voltage of very low frequency. Relative voltages for

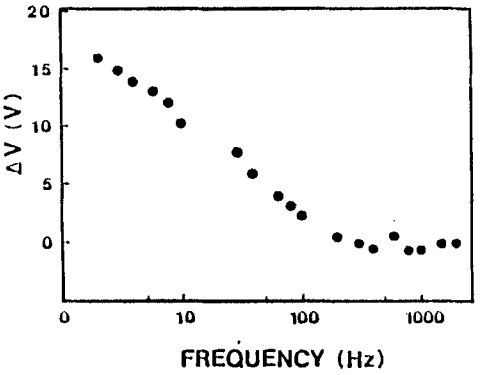

FIGURE 10 Frequency dependence of the internal ionic field in a CTC-doped SSFLC compared with an undoped one.

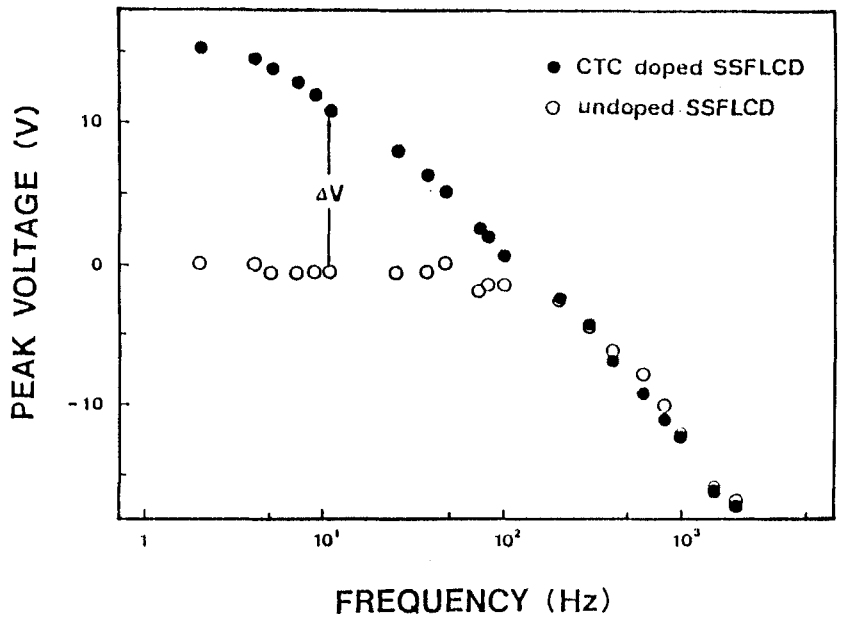

FIGURE 11 Relative voltages for the points of peaks for both CTC-doped (●) and undoped (○) samples as a function of the frequency of the applied triangular voltage.

the points of peaks for both samples are plotted against the frequency of the applied triangular voltages; the two lines coincide above 200 Hz.

The initiation of the reversal current occurs when the effective field E in the FLC medium changes its sign. Referring to an equation derived by Chieu and Yang[7]

$$E = \frac{V_0}{d + 2d'(\varepsilon/\varepsilon')} - \left[\frac{2d'/\varepsilon'}{(d/\varepsilon) + (2d'/\varepsilon')}\right]\left[\frac{\sigma(t) + P_s}{\varepsilon}\right],$$

where ε', and d' are the dielectric constant and the thickness of the alignment layers, ε, and d are the dielectric constant and the thickness of the FLC layer, V_0, $\sigma(t)$ and P_s are the applied voltage across the FLC cell, the ionic surface charge density and the bulk spontaneous polarization density, respectively.

One obtains surface charge density as

$$\sigma(t) = \frac{V_0\varepsilon'}{2d'} - P_s$$

giving rise to a zero effective internal field. The values for 0 are shown to range about 30 to 80 nC/cm^2.

The relative voltages corresponding to the peaks for the doped sample depend on the amplitudes of the triangular waveforms; they increase linearly in the low voltage region but tend to saturate in the higher voltage region as exemplified by the data of Figure 12.

From these facts, the occurrence of the inverted BS can be explained by the buildup of the depolarization field which needs a time duration of several hundreds of microseconds.

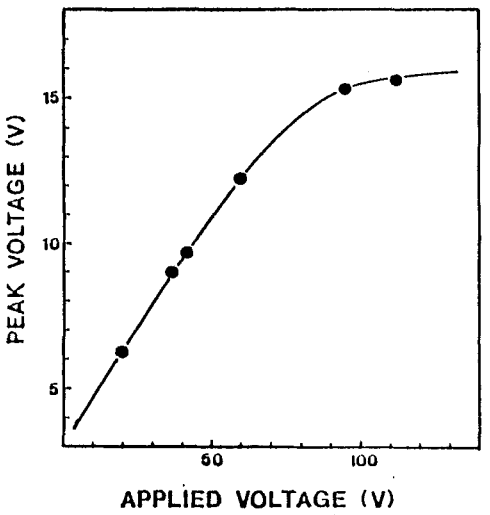

FIGURE 12 The peak voltage V_p as shown in Figure 7 plot against the applied triangular wave voltage V_{p-p} in the same frequency for CTC-doped SSFLC cell.

CONCLUSION

The effect of inverted bistability was brought about by the internal depolarization field which was caused by the surface ionic charges of CTC ions in the interfacial regions under the applied voltage in the cells. A new method for determining the internal ionic field has been discussed, and the results of the transient currents through the cell show two peaks originating from Ps and ions. The current peak of the ions is the so-called ionic hump. The average mobility of TMTTF or ODTCNQ ions obtained was 5×10^{-7} cm^2/V · s, a value lower than that expected for ions having a low molecular weight. This low mobility yields a long relaxation time keeping the internal depolarization fields for a time which is enough to yield the inverted bistability.

References

1. N. A. Clark and S. T. Lagerwall, *Appl. Phys. Lett.*, **36**, 899 (1980).
2. K. Skarp and M. A. Handschy: The 100th Anniversary of Liquid Crystal Research, ed. S. Kobayashi, *Mol. Cryst. & Liq. Cryst.*, **165**, 439 (1988).
3. H. Ikeno, Oh-saki, N. Ozaki, M. Nitta, K. Nakaya and S. Kobayashi, Society for Information Display International Symposium, Anaheim, CA, May 1988, Digest of technical Paper (SID, California, 1988), 45.
4. K. Nakaya, B. Y. Zhang, M. Yoshida, I. Isa, S. Shinoh and S. Kobayashi: *Jpn. J. Appl. Phys. Lett.*, **28**, L116 (1988).
5. M. Nitta, N. Ozaki, H. Suenaga, K. Nakaya and S. Kobayashi: *Jpn. J. Appl. Phys. Lett.*, **27**, L477 (1988).
6. K. H. Yang, T. C. Chieu and S. Osofsky: *Appl. Phys. Lett.*, **55**(2), 125 (1989).
7. T. C. Chieu and K. H. Yang: *Jpn. J. Appl. Phys.*, **28**, No. 11, Nov., 2240 (1989).
8. J. Vaxiviere, B. Labroo and P. H. Martinot-Lagarde: *Mol. Cryst. and Liq. Cryst.*, **172**, 61 (1989).
9. E. B. Priestley, P. J. Wojtowicz and P. Sheng: *Introduction to Liquid Crystals*, 319 (1974).
10. B. Y. Zhang, M. Yoshida, H. Sekine, C. M. Gomes, L. Chen and S. Kobayashi, *15th Japan Domestic Liquid Crystal Symposium*, **3A09**, 286 (1989), in Japanese.
11. B. Y. Zhang, M. Yoshida, H. Sekine and S. Kobayashi, *IEICE Technical Report*, **EID89-41**, 1 (1989), in Japanese.